VIBRATION MONITORING OF UH-60A MAIN TRANSMISSION PLANETARY CARRIER FAULT

Jonathan A. Keller
jonathan.keller@rdec.redstone.army.mil
U.S. Army AMCOM
Aviation Engineering Directorate
Redstone Arsenal, AL 35898-5000

Paul Grabill
paul.grabill@iac-online.com
Intelligent Automation Corporation
Poway, CA 92064

A crack in the planetary carrier of a UH-60A Blackhawk main transmission was investigated through analysis of the measured vibration time synchronous average. Vibration measurements of faulted and non-faulted transmissions were acquired at a range of torque settings in a controlled test cell environment and on-aircraft conditions. Several standard diagnostic parameters were modified for the special case of an epicyclic gearbox and applied to the measured data. Only two of the diagnostic parameters investigated in this paper were consistently successful at detecting the presence of a fault in test cell conditions. None of the diagnostic parameters were able to detect the crack in the on-aircraft conditions, measured only at low torque.

Notation

a	Amplitude modulation due to planet passage
b	Gear mesh vibration
d	Difference signal
f	Frequency
$\mathscr{F}$	Fourier transform
i,I	Index and total number of samples
j,J	Index and total number of averages
m,M	Index and total number of gear mesh harmonics
n,N	Index and total number of shaft harmonics
n_p,N_p	Index and total number of planets
N_t	Number of teeth in ring gear
Q	Rotor system torque
r	Regular signal
s	Residual signal
t,T	Time and sampling period
x	Time averaged vibration signal
y	Raw vibration signal
τ	Planet phase angle
$(\,)^e$	Epicyclic gearbox
$(\,)^g$	Fixed axis gearbox
$(\,)^s$	Shaft
$(\,)^{sb}$	Sideband

Introduction

Many rotorcraft main transmission systems are constructed using an epicyclic, or "planetary", gear train. Planetary gear trains consist of an inner "sun" gear, which is surrounded by two or more rotating "planets". The planets then also rotate inside the outer ring gear, which is usually stationary. Torque is transmitted through the sun gear to the planets, which ride on a planetary carrier. The planetary carrier, in turn, transmits torque to the main rotor shaft and blades.

Presented at the American Helicopter Society 59th Annual Forum, Phoenix, Arizona, May 6 – 8, 2003.

The H-60 main transmission employs a 5-planet epicyclic gear train. Recent inspections of two Army UH-60A Blackhawk main transmissions, initiated by indications of low or fluctuating oil pressure, revealed a crack in the planetary carriers. This is the first time this problem has been encountered in approximately 3.6 million UH-60A flight hours in the Army. The 10-inch crack in the first carrier, which was later cut apart for material inspection, is shown in Figure 1. Since the planetary carrier is a flight critical part, failure could cause an accident resulting in loss of life and/or aircraft. This resulted in flight restrictions on a significant number of Army UH-60A's. Manual inspection of all 1000 transmissions is not only costly in terms of labor, but also time prohibitive. A simple, cost-effective test capable of diagnosing this fault is highly desirable.

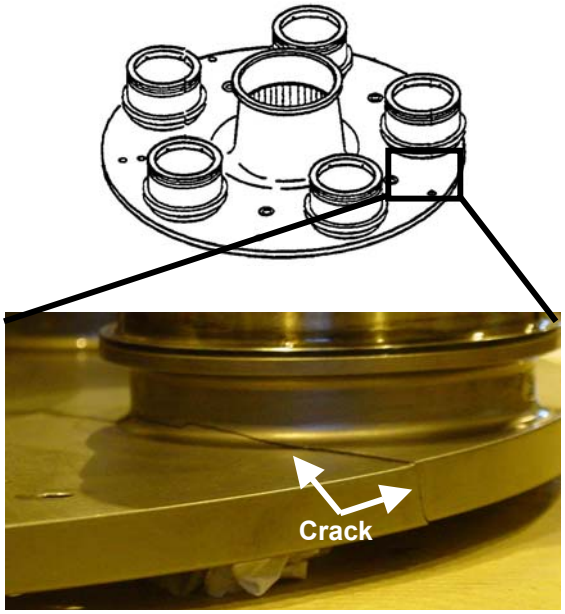

Figure 1. Planetary Carrier Schematic and Crack

Related Research

The analysis of vibration data to detect damage in fixed axis gears has been the focus of much research and experimentation. Gear health is typically described in terms of a single number, called a condition indicator (CI). The majority of CIs for fixed axis gears are developed by time synchronous averaging the vibration signal for the gear of interest. In this method, the vibration signal is measured by an accelerometer mounted on the gearbox housing and the raw vibration signal is time-averaged over numerous rotations with a pulse signal synchronized to the rotation of the gear. Random vibrations, which are asynchronous with the rotation of the gear, tend to average out. Stewart [1], Swansson [2], Favaloro [3], Martin [4] and Szczepanik [5] developed the first CIs using the time-averaged signal. Zakrajsek, Decker *et al* [6-9] developed evolutionary CIs using the time-averaged signal excluding particular shaft or gear mesh frequencies. More recently, Polyshchuk *et al* [10] have developed CIs using demodulation techniques originally proposed by McFadden [11].

As stated earlier, these CIs were developed to detect damage in fixed axis gear systems. For an accelerometer mounted to the housing, damage to individual gear teeth modulates the vibration signal at the shaft frequency. In the frequency domain, the damage appears in the form of symmetric sidebands around the gear meshing frequency, which is still the dominant component. The sidebands are located at integer multiples of the shaft frequency. Many of the CIs for fixed axis gears detect damage based upon the signal amplitude at the gear meshing frequency and/or modulating sidebands.

The measured vibrations produced by epicyclic gear systems are fundamentally different from fixed axis gear systems. An accelerometer mounted to the housing will measure a periodic amplitude-modulated vibration signal as each planet rotates past the sensor. Thus, even healthy gears will produce a vibration spectrum resulting in naturally occurring sidebands. Furthermore, because the vibrations produced by the planets are generally not in phase the dominant frequency component often does not occur at the fundamental gear meshing frequency. In fact, the gear meshing frequency component is often completely suppressed. This phenomenon was first recognized and explained by McFadden and Smith [12] and later McNames [13]. Thus, the CIs developed for fixed axis gears will give erroneous results even for an undamaged epicyclic gearbox. Clearly, the CIs require modification for application to an epicyclic gearbox. McFadden [14], Blunt and Hardman [15] and Pines [16] have also conducted research and experimentation on vibration monitoring of faults in individual planets of epicyclic gearboxes using windowing techniques.

Objectives

The U.S. Army Aviation Engineering Directorate, Aeromechanics Division conducted an investigation to determine if a fault in the planetary carrier of an H-60 transmission could be successfully detected via vibration monitoring. Experimental measurements of H-60 transmissions with both faulted and unfaulted planetary carriers were taken in a test cell and on-aircraft. In this paper, the several CIs for fixed axis gears are modified for the special case of an epicyclic gearbox and used to compare the vibration levels of known faulted and non-faulted transmissions.

Approach

Epicyclic Gearbox Vibrations

A brief explanation of the asymmetric sidebands produced by epicyclic gearboxes, based on McFadden [12], is presented here for reference. The gear mesh vibration produced by each planet can be expressed as

$$b_{n_p}(t) = \sum_{m=1}^{\infty} \beta_m \sin\left(mN_t\tau_{n_p}\right) \tag{1}$$

Where the phase for each planet is

$$\tau_{n_p} = 2\pi\left(f^s t + \frac{n_p - 1}{N_p}\right) \tag{2}$$

As the planets periodically rotate past the sensor, the vibration is modulated at the shaft frequency

$$a_{n_p}(t) = \sum_{n=0}^{\infty} \alpha_n \cos\left(n\tau_{n_p}\right)$$

The measured vibration in the fixed frame is the sum of the vibration from the individual planets

$$y(t) = \sum_{n_p=1}^{N_p} a_{n_p} b_{n_p} \tag{3}$$

Using the trigonometric identity

$$\sin A\cos B = \tfrac{1}{2}\sin(A+B) + \tfrac{1}{2}\sin(A-B) \tag{4}$$

Yields

$$y(t) = \tfrac{1}{2}\sum_{n_p=1}^{N_p}\sum_{m=1}^{\infty}\sum_{n=0}^{\infty}\alpha_n\beta_m \begin{Bmatrix} \sin\left[\left(mN_t + n\right)\tau_{n_p}\right] + \\ \sin\left[\left(mN_t - n\right)\tau_{n_p}\right] \end{Bmatrix} \tag{5}$$

The time-averaged signal is then

$$x(t) = \frac{1}{J}\sum_{j=1}^{J} y\left(t + jT^s\right) \tag{6}$$

The frequency content of the time-averaged signal can be found using the Fourier Coordinate Transform. Only terms with frequencies $mN_t \pm n$ that are multiples of the number of planets, N_p, are measured by a sensor in the fixed frame

$$f^e_{m,n} = \phi_{m,n}\left(mN_t \pm n\right) f^s$$

$$\phi_{m,n} = \begin{cases} 1 & if \quad \frac{mN_t \pm n}{N_p} = \text{integer} \\ 0 & if \quad \frac{mN_t \pm n}{N_p} \neq \text{integer} \end{cases} \tag{7}$$

In contrast, for a fixed axis gearbox the gear meshing frequencies simply occur at

$$f_m^g = mN_t f^s \tag{8}$$

The computed frequency spectra around the fundamental gear mesh for a "damaged" and an undamaged H-60 main transmission (N_p = 5, N_t = 228) are shown in Figure 2. For the undamaged transmission, the gear meshing component at n = 0 (order 228) is almost completely suppressed but several apparent meshing frequencies occur naturally at n = -3, +2 and +7. The largest amplitude, or dominant, component at n = +2 occurs closest to the gear mesh frequency. For the "damaged" transmission, it is assumed that one planet generates a vibration signal of different amplitude than the other planets. This assumption is for demonstrative purposes only; it is not used for data analysis. This results in the reappearance of the gear meshing component and larger sidebands around the apparent frequency components.

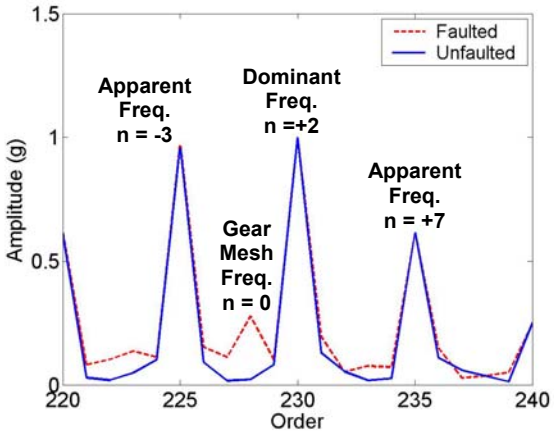

Figure 2. Simulated H-60 Main Transmission Vibration Spectra

Modified Condition Indicators

In this section, only the CIs requiring modification for the special case of an epicyclic gearbox are presented. Standard definitions are in Refs. 1-5.

Regular Mesh Components. Many of the CIs for fixed axis gears are based on the time signal average excluding "regular" mesh components, RMC. These "regular" components are defined as the fundamental shaft frequency, the fundamental and harmonics of the gear meshing frequency and their first order sidebands. The first order sidebands are generally due to run-out of the gear because of machining or assembly inaccuracies [17] and thus can be considered regular components.

Because of the asymmetry effect in the frequency spectrum for an epicyclic gearbox, Eqn. (7) must be used to identify analogous frequency components. For an epicyclic gearbox the "regular" mesh components are defined as the fundamental shaft frequency, all the apparent gear mesh frequency components for each harmonic and the first-order sidebands of the dominant gear mesh frequency for each harmonic.

$$\begin{aligned} \mathrm{RMC}^s(x) &= \mathscr{T}[x]\big|_{f^s} \\ \mathrm{RMC}^e_{m,n}(x) &= \mathscr{T}[x]\big|_{f^e_{m,n}} \\ \mathrm{RMC}^{esb}_{m,n_{\text{dominant}}\pm 1}(x) &= \mathscr{T}[x]\big|_{f^e_{m,n_{\text{dominant}}}\pm f^s} \end{aligned} \tag{9}$$

Regular, Difference and Residual Signals. The regular signal is defined as the inverse Fourier transform of the regular mesh components. The difference signal is defined as the time signal average excluding the regular mesh components. The residual signal is similar to the difference signal, but includes the first-order sidebands of the dominant gear mesh frequency.

$$\begin{aligned} r^e &= \mathscr{T}^{-1}\left[\mathrm{RMC}^s(x)+\mathrm{RMC}^e(x)+\mathrm{RMC}^{esb}(x)\right] \\ d^e &= x - r^e \\ s^e &= x - \mathscr{T}^{-1}\left[\mathrm{RMC}^s(x)+\mathrm{RMC}^e(x)\right] \end{aligned} \tag{10}$$

Zero-Order Figure of Merit. For a fixed axis gearbox, the zero-order Figure of Merit, FM0, is defined as the peak-to-peak value of the time-averaged signal normalized by the sum of amplitudes of the regular mesh frequencies [1]. For an epicyclic gearbox FM0^e is defined using the dominant mesh frequencies.

$$\mathrm{FM0}^e = \frac{\max(x)-\min(x)}{\sum_{m=1}^{M}\mathrm{RMC}^e_{m,n_{\text{dominant}}}(x)} \tag{11}$$

Energy Ratio. For a fixed axis gearbox, the energy ratio, ER, is defined as the standard deviation of the difference signal normalized by the standard deviation of the regular signal [2]. For an epicyclic gearbox the energy ratio, ER^e, is defined using the appropriately calculated difference and regular signals.

$$\mathrm{ER}^e = \frac{\mathrm{RMS}(d^e)}{\mathrm{RMS}(r^e)} \tag{12}$$

Sideband Level Factor. For a fixed axis gearbox, the sideband level factor, SLF, is defined as the sum of the first-order sideband amplitudes about the fundamental gear meshing frequency normalized by the standard deviation of the time signal average [3]. For an epicyclic gearbox the sideband level factor, SLF^e, is defined using the first-order sideband amplitudes about the fundamental dominant meshing component.

$$\mathrm{SLF}^e = \frac{\mathrm{RMC}^{esb}_{1,n_{\text{dominant}}-1}(x)+\mathrm{RMC}^{esb}_{1,n_{\text{dominant}}+1}(x)}{\mathrm{RMS}(x)} \tag{13}$$

Sideband Index. For a fixed axis gearbox, the sideband index, SI, is defined as the average amplitude of the sidebands of the fundamental gear meshing frequency [5]. For an epicyclic gearbox the sideband index, SI^e, is defined using the only the first-order sidebands of the fundamental dominant frequency component.

$$\mathrm{SI}^{e} = \frac{\mathrm{RMC}^{esb}_{1,n_{\mathrm{dominant}}-1}(x) + \mathrm{RMC}^{esb}_{1,n_{\mathrm{dominant}}+1}(x)}{2} \quad (14)$$

Normalized Kurtosis. The normalized Kurtosis, NK, is a standard statistical definition. It is defined as the fourth statistical moment of the signal about the mean of the signal (or absolute Kurtosis, AK) normalized by the square of the variance of the signal [18].

$$\mathrm{NK}(x) = \frac{\mathrm{AK}(x)}{\left[\sigma^2(x)\right]^2} = \frac{I\sum_{i=1}^{I}(x_i - \bar{x})^4}{\left[\sum_{i=1}^{I}(x_i - \bar{x})^2\right]^2} \quad (15)$$

Fourth-Order Figure of Merit. For a fixed axis gearbox the normalized Kurtosis of the difference signal has been termed FM4 [1]. "Good" gearboxes have a near Gaussian amplitude distribution of the vibration, resulting in a normalized Kurtosis of nearly 3. For an epicyclic gearbox, $\mathrm{FM4}^{e}$ is defined using the appropriately calculated difference signal.

$$\mathrm{FM4}^{e} = \mathrm{NK}\left(d^{e}\right) \quad (16)$$

CIs similar to FM4 such as FM4*, NA4, NA4*, NB4 and NB4* have also been proposed [6-9]. These CIs use the residual or analytic signals and are normalized by a running average of the variance, which may even be "locked" when it reaches a predefined limit. However, these CIs are not the subject of this paper because they require vibration data for an extended period of time as the gearbox accrues damage.

Experimental Testing

Test Cell Measurements. The Helicopter Transmission Test Facility (HTTF) at Patuxent River NAS, MD was utilized for all test cell measurements. The HTTF is a unique test facility that uses actual aircraft engines to provide power to all the aircraft drive systems except the rotors and is a significant improvement over single component test rigs [19-20]. An H-60 test transmission was instrumented with several sets of accelerometers. A list of the accelerometers and their locations is included in Table 1 and shown in Figure 3.

Table 1. Accelerometers

No.	Name	Location	Axis
1	ACC GBX 1	Left Accessory Module	Vert.
2	ACC GBX 2	Right Accessory Mod.	Vert.
3	INPT GBX 1	Left Input Module	Vert.
4	INPT GBX 2	Right Input Module	Vert.
5	MAIN 1	Main Module, Left Side	Rad.
6	MAIN 2	Main Module, Right Side	Rad.

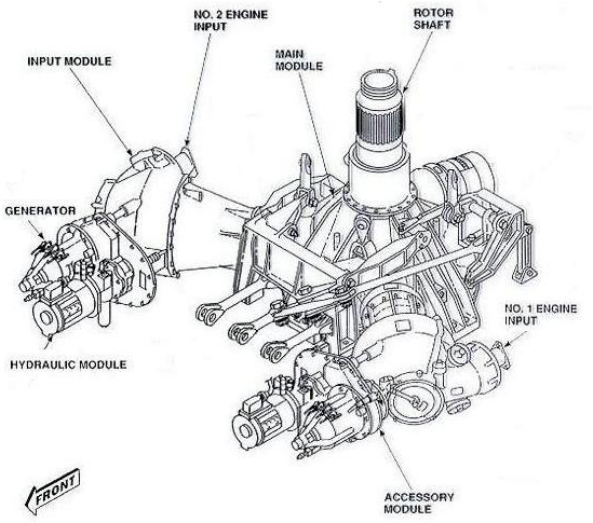

a) Isometric View

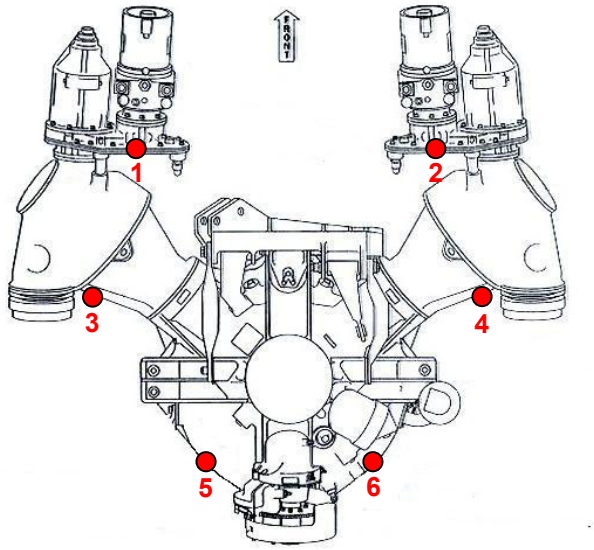

b) Top View

Figure 3. H-60 Transmission and Sensor Locations

The vibration data was acquired using the US Army's Vibration Management Enhancement Program (VMEP) system. Measurement setups were created to simultaneously acquire and synchronize the six input accelerometers to the carrier rotational frequency. The VMEP system was programmed to calculate and save the raw time domain data, the time synchronous waveform, and the condition indicators. A list of the VMEP setup parameters is included in Table 2. Time synchronous vibration data were measured for each accelerometer at torque settings ranging from 20% to 100%. Both faulted and unfaulted planetary carriers were tested. The faulted planetary carrier, the second cracked UH-60A carrier discovered during a field inspection, had a 3¼-inch crack when installed in the test transmission. Because of the need for destructive material testing on the cracked carrier, the amount of

run time was limited. Thus, the transmission was not run for an extended period. Only "snapshots" of data at each torque setting were measured.

Table 2. Data Acquisition and Processing

Data Type	Parameters
Input	Accelerometers: 6
	Sample rate: 48 KHz
	Tachometers: 1
Asynchronous Time Domain (ATD)	Save to File: yes
	Number of Points: 1,200,000
Synchronous Time Average (STA)	Save to File: yes
	Target shaft: planet carrier
	Revs averaged: 80
	Points per rev: 8192
Asynchronous Frequency Domain (AFD)	Save to file: yes
	f_{max}: 2000 Hz
	Points per AFD: 6400
	Number of Averages: 10
	Window: Flat Top
	Overlap: 50%

On-Aircraft Measurements. Similar to the test cell measurements, several UH-60A transmissions were instrumented. However, for the on-aircraft tests only accelerometers 3 through 6 were used. Time synchronous vibration data were measured for each accelerometer using the same data acquisition equipment that was used in the test cell. The same faulted carrier and main gearbox used in the tests at the HTTF was installed in a UH-60A at the Corpus Christ Army Depot (CCAD) and used as a test aircraft. Three different UH-60As from the Birmingham, Alabama National Guard (BNG) with unfaulted carriers were selected as test aircraft to establish how vibration levels change across aircraft. Because of safety issues with the cracked carrier only ground runs were completed. Single and dual engine data were taken at torque settings of 20%*Q* and 30%*Q*. For each test state, the aircraft was stabilized for 5 minutes before vibration measurements were taken. For all tests, winds were less than 10 knots with the nose of the aircraft pointed into the wind.

Sample Results

Time Synchronous Averages (TSAs)

Example TSAs measured by accelerometer 5 (left main module) at 30%*Q* are shown in Figure 4 for the test cell measurements. Both the gear meshing frequency and the amplitude modulation effect as each of the 5 planets pass the accelerometer is easily identifiable. Also note the amplitudes are slightly larger for the faulted carrier. The same measurements taken on-aircraft are shown in Figure 5. The planet passage effect is not nearly as noticeable as in the test cell measurement. Also, in this case the aircraft with an unfaulted carrier resulted in higher amplitude vibration than the aircraft with the faulted carrier. Clearly a faulted carrier will be much more difficult to detect in field conditions than in the controlled test cell environment.

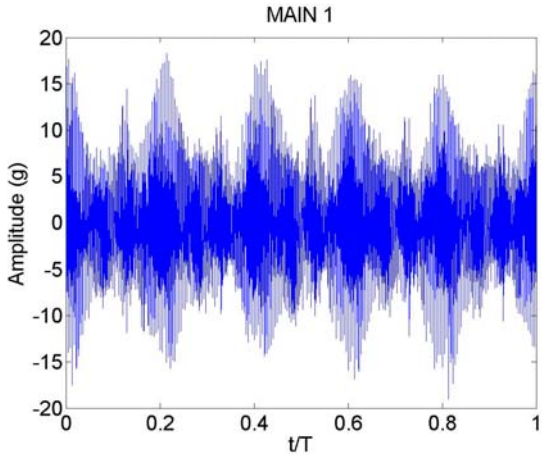

a) Unfaulted

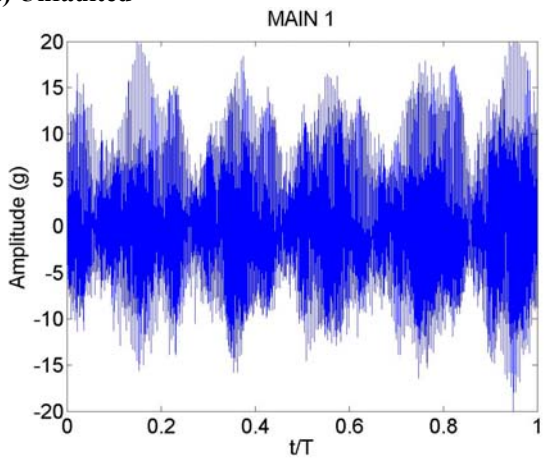

b) Faulted

Figure 4. Test Cell TSAs (Left Main, 30%*Q*)

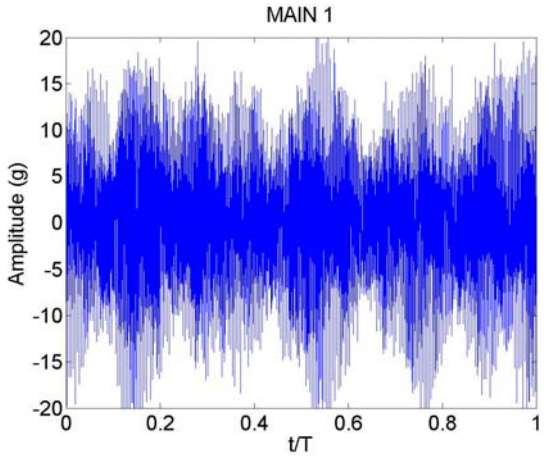

a) Unfaulted

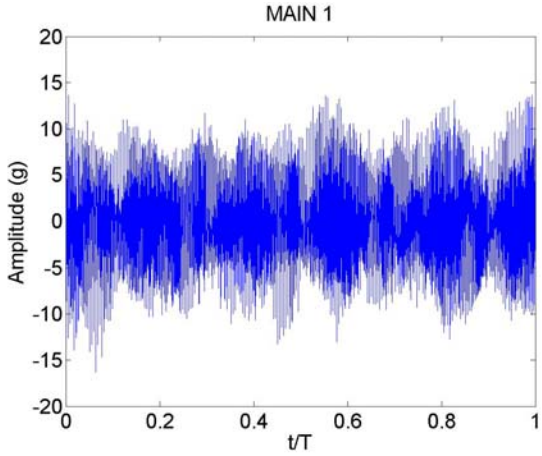

b) Faulted

Figure 5. On-Aircraft TSAs (Left Main, 30%Q)

Synchronous Order Domain (SOD) spectra were calculated using the synchronous time averaged waveforms saved by the data acquisition system. Example spectra for the test cell and on-aircraft measurements are shown in Figure 6 and Figure 7. For the test cell measurements, the unfaulted carrier only has significant amplitude the apparent frequencies predicted by Eqn. (7) at n = -3, +2 and +7 (orders 225, 230 and 235). In contrast, the faulted carrier has increased energy at the n = -1, 0, +1 and +3 sidebands around the dominant sideband at n = +2.

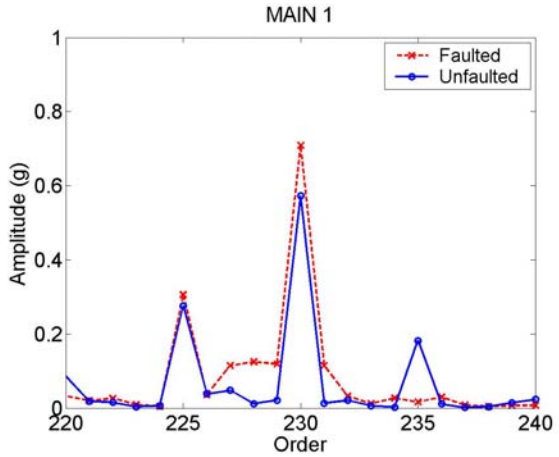

Figure 6. Test Cell Spectra (Left Main, 30%Q)

For the on-aircraft measurements, the situation is not as clear. For the unfaulted carrier, the dominant apparent sideband is no longer at n = +2 but at n = -3. Also, relative to the amplitude of the n = +2 and –3 sidebands the unfaulted carrier has significant amplitudes at the n = +1 sideband. For the faulted carrier, the n = +2 sideband is still dominant and significant energy at the n = -1, 0 and +1 sidebands is apparent. Visual inspection of the spectra show that some condition indicators may incorrectly indicate the presence of a fault in the unfaulted, on-aircraft data.

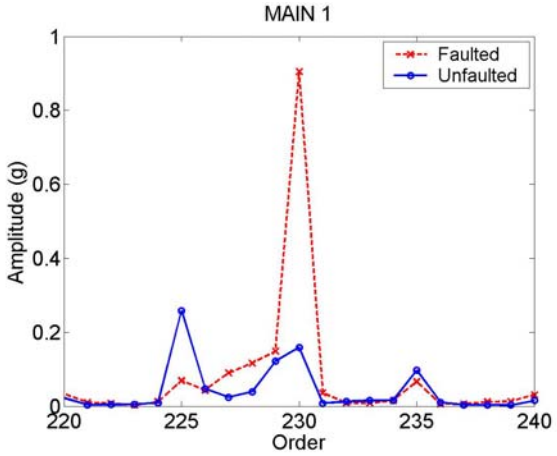

Figure 7. On-Aircraft Spectra (Left Main, 30%Q)

<u>Modified Condition Indicators</u>

In this section, the sample results for some standard condition indicators and the condition indicators modified for the special case of an epicyclic gearbox are presented. Each condition indicator is shown as a function of rotor system torque for the sensor of interest. Test cell and on-aircraft measurements are shown separately for clarity.

The normalized Kurtosis of the time synchronous average for accelerometer 5 (left main module) is shown in Figure 8. For the test cell measurements, the NK for both the faulted and unfaulted gearboxes ranges from 2.4 to 3.2. The value of 3.0 expected for a "normal" gearbox is shown as a dashed line. For the 20% and 30% torque settings, the unfaulted carrier has the higher NK. For all other torque settings, the faulted carrier has the higher NK. For the on-aircraft measurements, most NK values range from 2.5 to 3 while two unfaulted measurements have increased NK values of nearly 4. However, the faulted measurements all have NK values of 2.5 to 2.6.

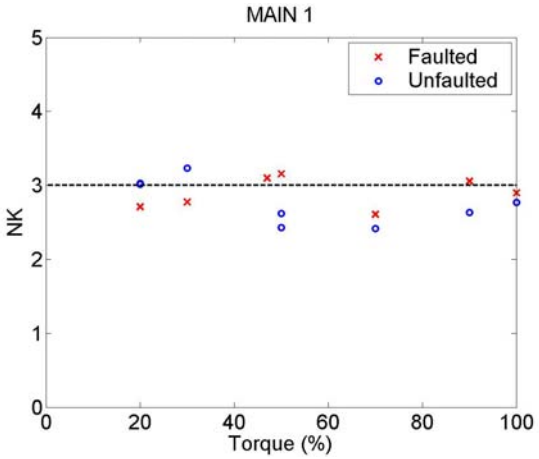

a) Test Cell

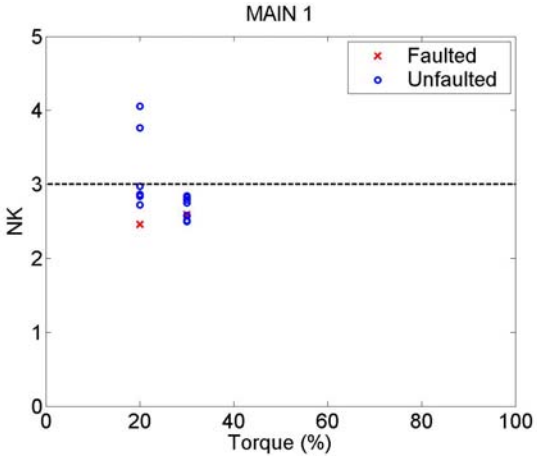

b) On-aircraft

Figure 8. Normalized Kurtosis (Left Main)

The Crest Factor (CF) of the time signal average for accelerometer 5 (left main module) is shown in Figure 9. The CF, defined as the maximum value of the TSA normalized by the RMS value, does not need to be modified for an epicyclic gearbox. For the test cell measurements, the CF for both the faulted and unfaulted gearboxes ranges between 2.5 and 4. For the on-aircraft measurements, the CF ranges between 2.8 and 4. In both figures, no consistent trend between faulted and unfaulted gearboxes is apparent.

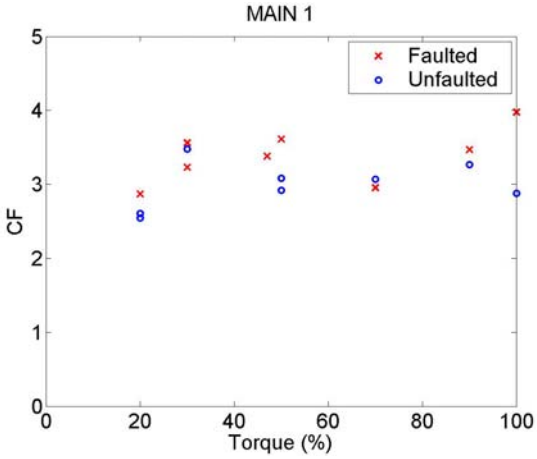

a) Test Cell

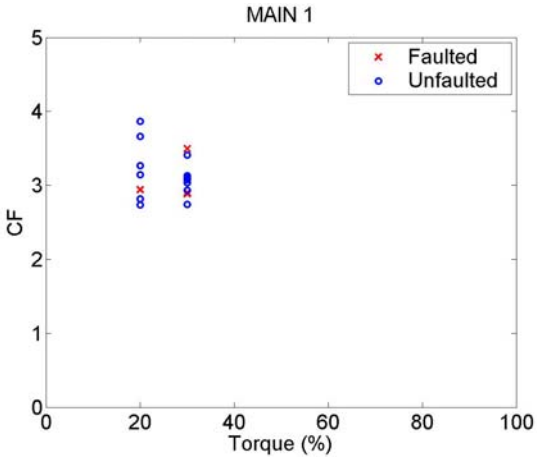

b) On-aircraft

Figure 9. Crest Factor (Left Main)

FM0^e for accelerometer 5 (left main module) is shown in Figure 10. For the test cell measurements, FM0^e ranges from 2.2 to 4. FM0^e is also consistently 10% to 40% larger for the faulted gearbox than for the unfaulted gearbox. For the on-aircraft measurements, FM0^e also ranges from 2.2 to 4; however, in almost all cases it is significantly larger for the unfaulted gearboxes than for the faulted gearbox.

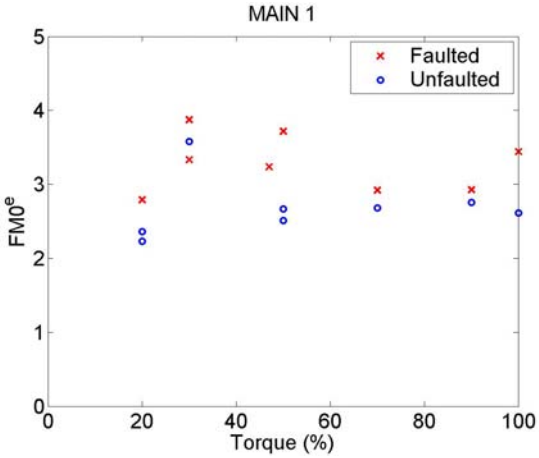

a) Test Cell

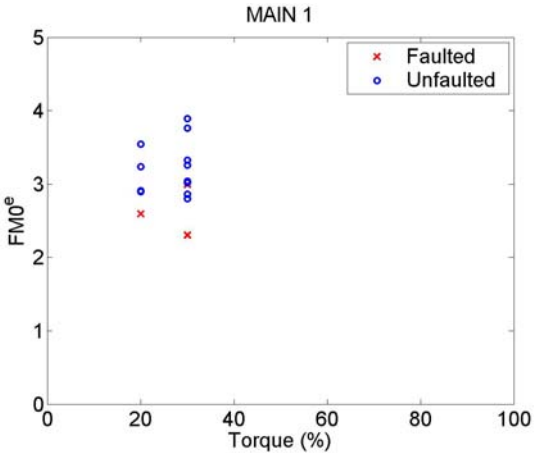

b) On-aircraft

Figure 10. FM0^e (Left Main)

FM0^e for accelerometer 3 (left input module) is shown in Figure 11. The results for the left input module are very similar to the left main module. FM0^e is consistently 10% to 50% larger for the faulted gearbox than for the unfaulted gearbox in the test cell measurements. FM0^e for the faulted 70%Q measurement even reaches a value of 7.8. But on-aircraft FM0^e for the faulted measurements is consistently lower than the unfaulted measurements. Some of the unfaulted measurements are as high as 8.

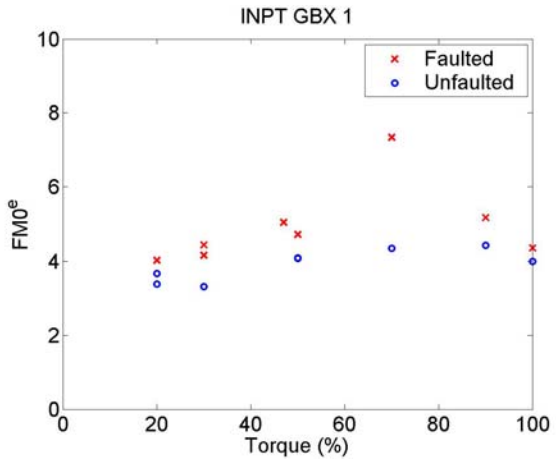

a) Test Cell

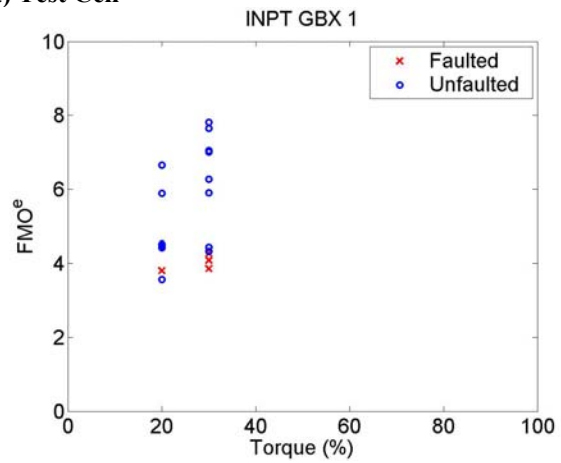

b) On-aircraft

Figure 11. FM0^e (Left Input)

The ER^e for accelerometer 2 (right input module) is shown in Figure 12. For the test cell measurements, the ER^e varies widely with torque. For the 90% and 100% torque settings, the faulted ER^e is approximately 2 times the unfaulted ER^e. For the on aircraft measurements, the ERE is larger for the unfaulted gearbox than the faulted gearbox for the majority of the test points.

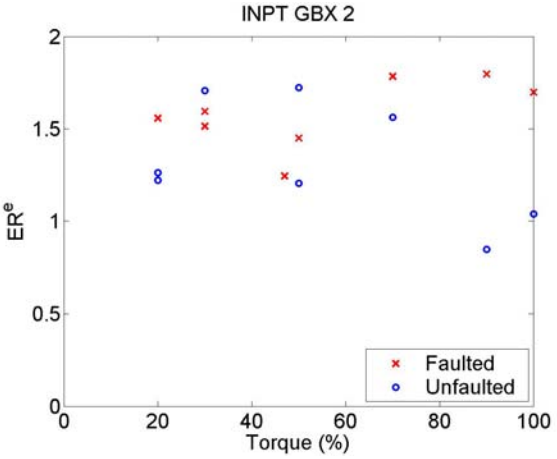

a) Test Cell

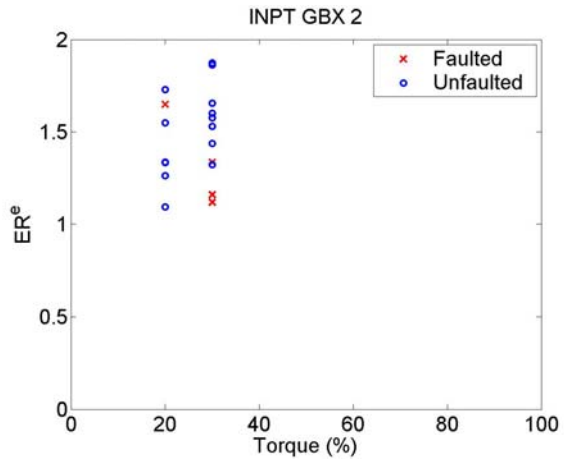

b) On-aircraft

Figure 12. ER^e (Right Input)

The SLF^e for accelerometer 5 (left main module) is shown in Figure 13. For the test cell measurements, the SLF^e is consistently larger for the faulted gearbox than for the unfaulted gearbox. However, for the on-aircraft measurements, the SLF^e is larger in almost all cases for the unfaulted gearboxes.

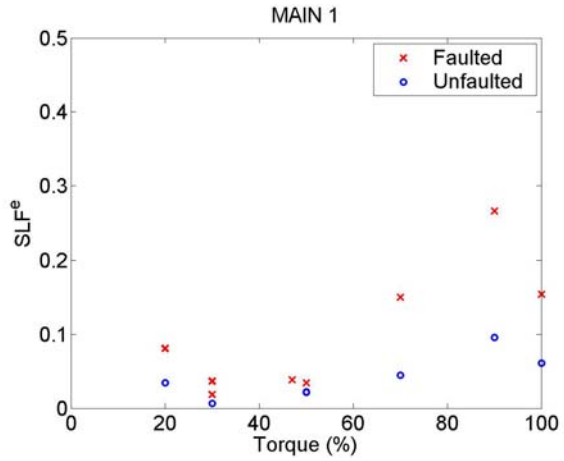

a) Test Cell

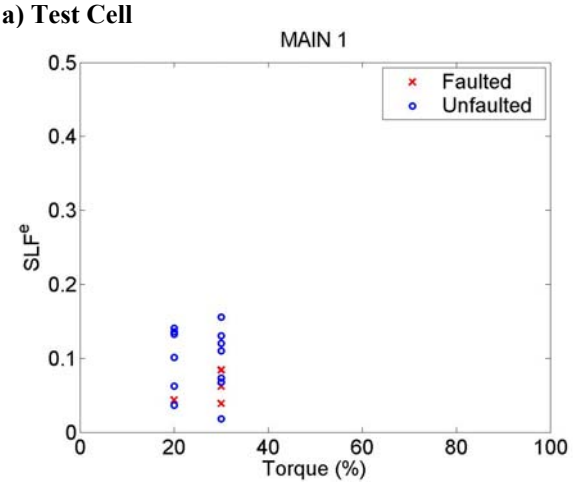

b) On-aircraft

Figure 13. SLF^e (Left Main)

Similarly, the SLF^e for accelerometer 4 (right input module) is shown in Figure 14. Once again for the test cell measurements, the SLF^e is consistently larger for the faulted gearbox than for the unfaulted gearbox, especially for the 20% and 30% torque settings. However, for the on-aircraft measurements, SLF^e is larger in almost all cases for the unfaulted gearbox measurements and shows a wide variation across aircraft, ranging from 0.05 to 0.35.

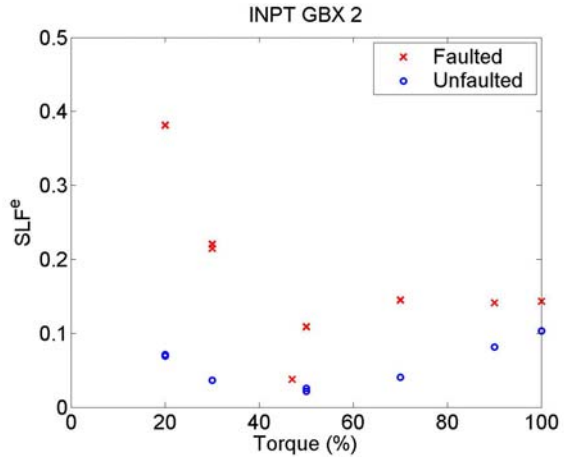

a) Test Cell

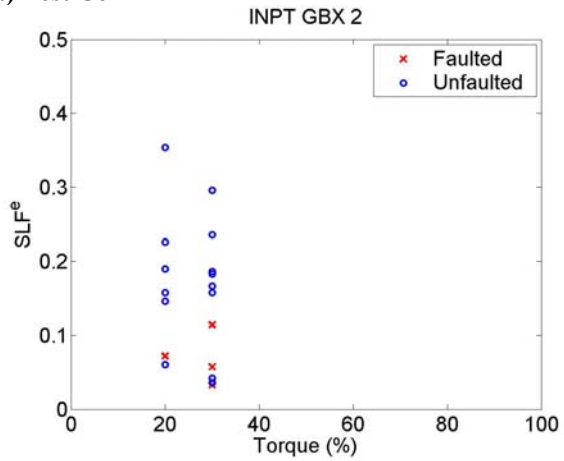

b) On-aircraft

Figure 14. SLF^e (Right Input)

The SI^e for accelerometer 5 (left main module) is shown in Figure 15. For the test cell measurements, the SI^e is consistently larger for the faulted gearbox than for the unfaulted gearbox, especially at the 90% and 100% torque settings. However, for the on-aircraft measurements, the SI^e is larger in almost all cases for the unfaulted gearboxes and again shows a wide variation from aircraft to aircraft, ranging from 0.05 to 0.45.

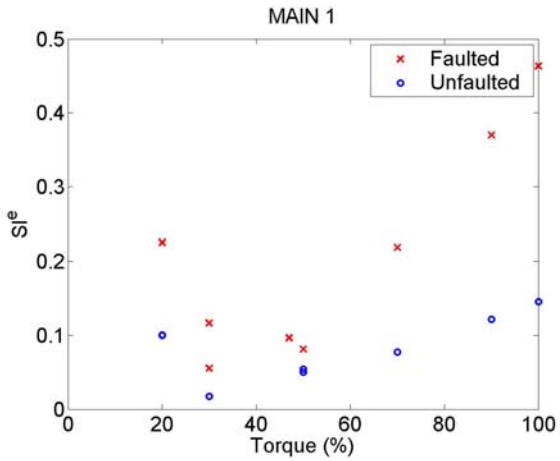

a) Test Cell

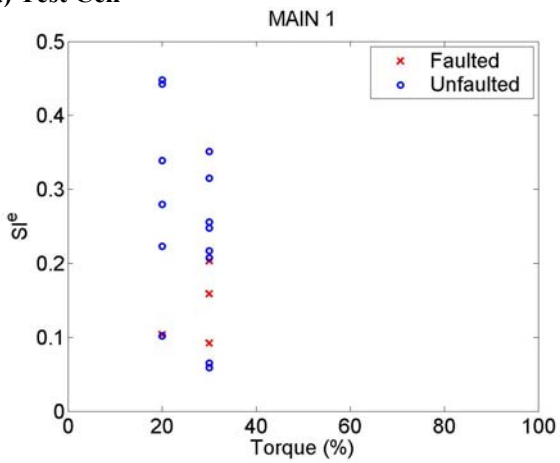

b) On-aircraft

Figure 15. SI^e (Left Main)

The SI^e for accelerometer 4 (right input module) is shown in Figure 16. For the test cell measurements, like the left main module, the SI^e is consistently larger for the faulted gearbox than for the unfaulted gearbox, especially at the 20% and 30% torque settings. However, for the on-aircraft measurements, the SI^e is again larger in almost all cases for the unfaulted gearboxes.

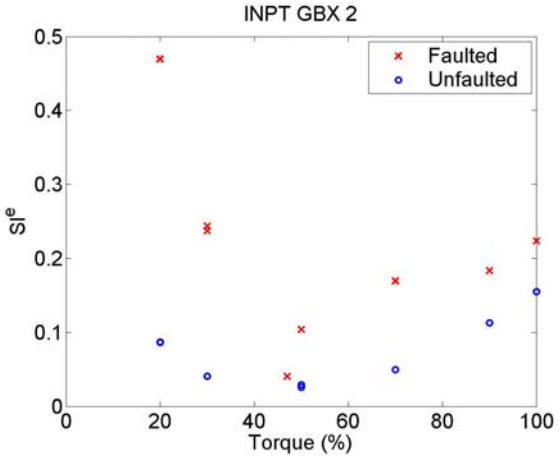

a) Test Cell

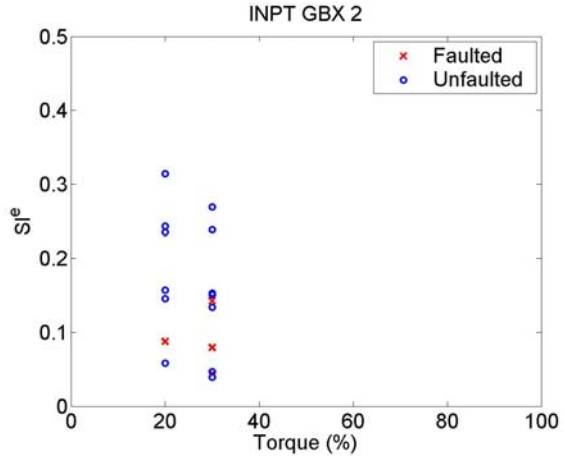

b) On-aircraft

Figure 16. SI^e (Right Input)

FM4^e for accelerometer 5 (left main module) is shown in Figure 17. For the test cell measurements, FM4^e for both faulted and unfaulted gearboxes ranges from 3.2 to 5.6. For the on-aircraft measurements, FM4^e for both faulted and unfaulted gearboxes ranges from 2.6 to 4.4. Neither shows a consistent pattern.

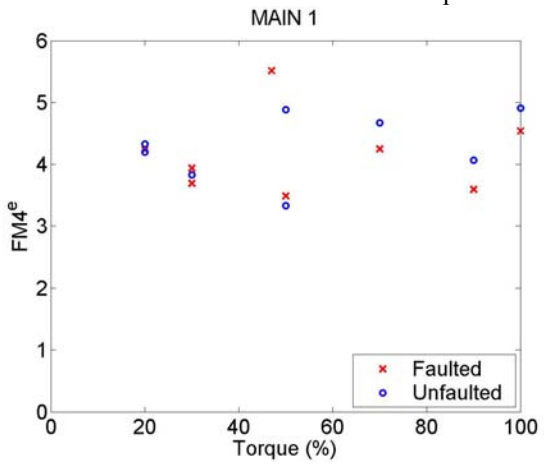

a) Test Cell

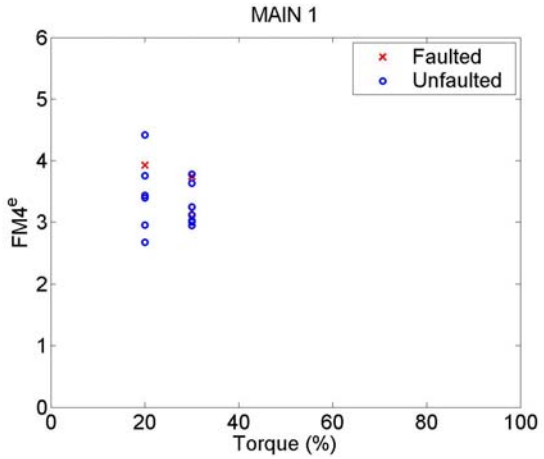

b) On-aircraft

Figure 17. FM4^e (Left Main)

Conclusions

A crack in the planetary carrier of a UH-60A Blackhawk main transmission was investigated with time synchronous averaging of the vibration measured at six different locations on the main, input and accessory gearboxes. Vibration measurements of faulted and non-faulted transmissions were acquired in a controlled test cell environment and on-aircraft conditions at torque levels from 20% to 100%. Several standard diagnostic parameters were modified for the special case of an epicyclic gearbox and applied to the measured data. Of the diagnostic parameters investigated in this paper, only the sideband index (SI) and sideband level factors (SLF) were consistently successful at detecting the presence of a fault in test cell conditions. None of the diagnostic parameters were able to detect a crack in on-aircraft conditions at the low torque levels tested. This indicates that a cracked carrier is detectable in controlled test cell conditions, but noise from other rotating components and differences in the vibration levels from aircraft-to-aircraft may overshadow the effect of a cracked planetary carrier. It is also possible that the low torque values of the on-aircraft testing were not sufficient to expose the fault.

Acknowledgments

The authors would like to thank the staff at the Helicopter Transmission Test Facility (HTTF) at Patuxent River, MD including Mr. Frank Dawson and Mr. William Hardman; Corpus Christi Army Depot and the Birmingham, Alabama National Guard for their help in the experimental testing. The authors would also like to thank Mr. Eric Bale, Mr. Ronald Bednarczyk, Mr. Robert Branhof and Dr. John Berry of USAAMCOM, AED, Redstone Arsenal, AL for assistance in gathering and analyzing the data.

References

1. Stewart, R.M., "Some Useful Data Analysis Techniques for Gearbox Diagnostics," Report MHM/R/10/77, Machine Health Monitoring Group, Institute of Sound and Vibration Research, University of Southampton, July 1977.
2. Swansson, N.S., "Application of Vibration Signal Analysis Techniques to Condition Monitoring," *Proceedings of the Conference on Friction and Wear in Engineering*, Institution of Engineers, Barton, Australia, Dec. 1980, pp. 262-267.
3. Favaloro, S.C., "A Preliminary Evaluation of Some Gear Diagnostics Using Vibration Analysis," ARL-AERO-PROP-TM-427, Aeronautical Research Laboratories, Department of Defence, Melbourne, Australia, July 1985.
4. Martin, H.R., "Statistical Moment Analysis as a Means of Surface Damage Detection," *Proceedings*

of the 7th International Modal Analysis Conference, Society for Experimental Mechanics, Schenectady, NY, Jan. 1989, pp. 1016-1021.
5. Szczepanik, A., "Time Synchronous Averaging of Ball Mill Vibrations," *Mechanical Systems and Signal Processing*, Vol. 3, No. 1, Jan. 1989, pp. 99-107.
6. Zakrajsek, J.J., Townsend, D.P., and Decker, H.J., "An Analysis of Gear Fault Detection Methods as Applied to Pitting Fatigue Failure Data," NASA TM-105950, Jan. 1993.
7. Decker, H.J., Handschuh, R.F., and Zakrajsek, J.J., "An Enhancement to the NA4 Gear Vibration Diagnostic Parameter," NASA TM-106553, June 1994.
8. Zakrajsek, J.J., Handschuh, R.F., and Decker, H.J., "Application of Fault Detection Techniques to Spiral Bevel Gear Fatigue Data," NASA TM-106467, Jan. 1994.
9. Decker, H.J., "Crack Detection for Aerospace Quality Spur Gears," *Proceedings of the AHS International 58th Annual Forum*, American Helicopter Society, June 2002.
10. Polyshchuk, V.V., Choy, F.K., and Braun, M.J., Gear Fault Detection with Time-Frequency Based Parameter NP4," *International Journal of Rotating Machinery*, Vol. 8, No. 1, Jan. 2002, pp. 57-70.
11. McFadden, P.D., "Detecting Fatigue Cracks in Gears by Amplitude and Phase Demodulation of the Meshing Vibration," *Journal of Vibration, Acoustics, Stress, and Reliability in Design*, Vol. 108, No. 2, Apr. 1986, pp. 165-170.
12. McFadden, P.D., and Smith, J.D., "An Explanation for the Asymmetry of the Modulation Sidebands about the Tooth Meshing Frequency in Epicyclic Gear Vibration," *Proceedings of the Institution of Mechanical Engineers, Part C: Mechanical Engineering Science*, Vol. 199, No. 1, Jan. 1985, pp. 65-70.
13. McNames, J., "Fourier Series Analysis of Epicyclic Gearbox Vibration," *Journal of Vibration and Acoustics*, Vol. 124, No. 1, Jan. 2002, pp. 150-152.
14. McFadden, P.D., "A Technique for Calculating the Time Domain Averages of the Vibration of the Individual Planet Gears and the Sun Gear in an Epicyclic Gearbox," *Journal of Sound and Vibration*, Vol. 144, No. 1, 1991, pp. 163-172.
15. Blunt, D.M., and Hardman, W.J., "Detection of SH-60 Helicopter Main Transmission Planet Gear Fault Using Vibration Analysis," Report No. NAWCADPAX/RTR-2000/123, Naval Air Warfare Center Aircraft Division, Patuxent River, MD, 2000.
16. Samuel, P., and Pines, D., "Planetary Gear Box Diagnostics using Adaptive Vibration Signal Representations: A Proposed Methodology," *Proceedings of the AHS 57th Annual Forum*, American Helicopter Society, May 2001.
17. Gu, A.L., and Badgley, R.H., "Prediction of Vibration Sidebands in Gear Meshes," ASME Paper 74-DET-95, Oct. 1974.
18. Miller, I., and Freund, J.E., Probability and Statistics for Engineers, 3rd Edition, Prentice-Hall, Inc., Englewood Cliffs, NJ, 1985.
19. Hardman, W., and Hess, A., "A USN Strategy for Mechanical and Propulsion Systems Prognostics with Demonstration Results," *Proceedings of the AHS 58th Annual Forum*, American Helicopter Society, June 2002.
20. Hardman, W., Hess, A., McGonigle, M., and Sheaffer, J., "An Update Status for the SH-60 Helicopter Integrated Diagnostic System (HIDS) Program – Diagnostic and Prognostic Experience," *Proceedings of the AHS 55th Annual Forum*, American Helicopter Society, May 1999, pp. 2349-2356.